Supplementary information

Interface-charge induced giant electrocaloric effect in lead free ferroelectric thin-film bilayers

Sagar E. Shirsath[1], Claudio Cazorla[1], Teng Lu[2], Le Zhang[1], Yee Yan Tay[3], Xiaojie Lou[4], Yun Liu[2], Sean Li[1] and Danyang Wang[1,*]

[1] *School of Materials Science and Engineering, UNSW Sydney, NSW 2052, Australia*

[2]*Research School of Chemistry, The Australian National University, ACT 2601, Australia*

[3]*Facility for Analysis, Characterization, Testing and Simulation and School of Materials Science and Engineering, Nanyang Technological University, 50 Nanyang Avenue, 639798 Singapore*

[4]*Multi-disciplinary Materials Research Centre, Frontier Institute of Science and Technology, and State Key Laboratory for Mechanical Behavior of Materials, Xi'an Jiaotong University, Xi'an 710049, China*

*Corresponding author: dy.wang@unsw.edu.au (DW)

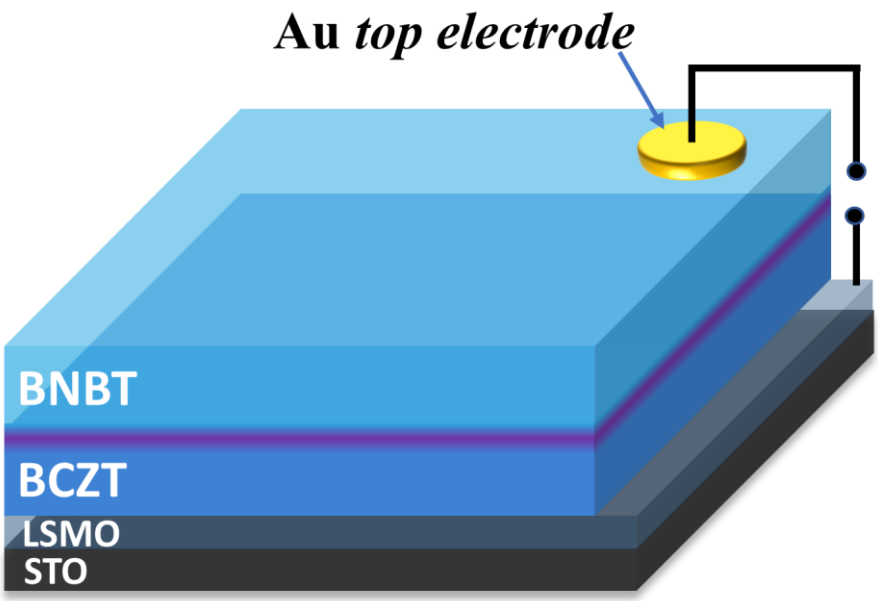

Figure S1: Schematic illustration of BNBT/BCZT bilayer thin films deposited on $SrTiO_3$ (STO) (001) single crystal substrate. Au and LSMO were used as a top and bottom electrode respectively.

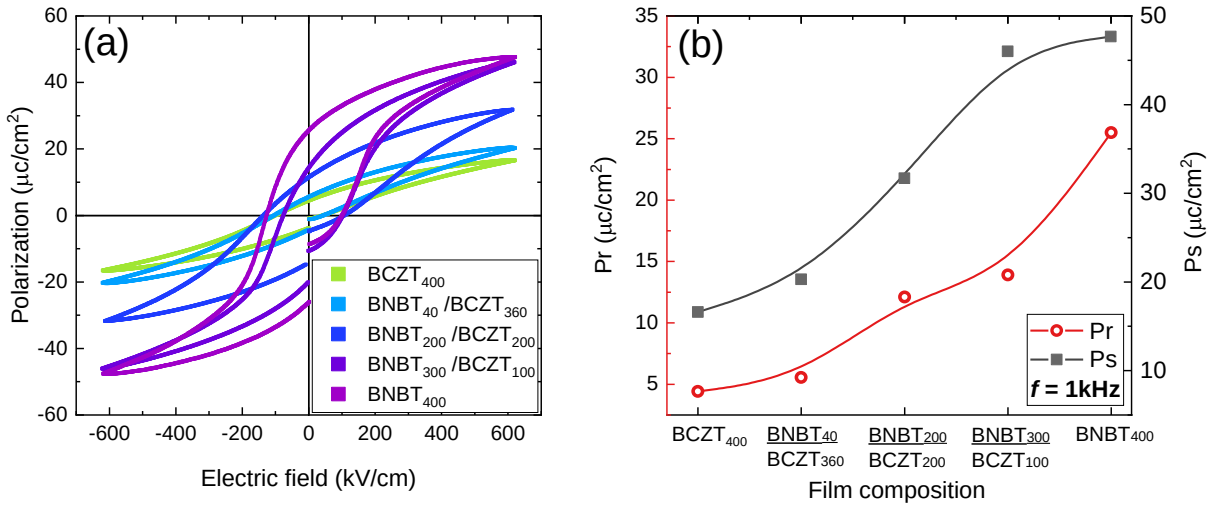

FigureS2:**a**,Room temperature polarization versus electric field (P-E) hysteresis loops of BNBT, BCZT and BNBT/BCZT bilayer thin films measured at f = 1 kHz. **b**, Saturation polarization (Ps) and remanent polarization (Pr) obtained from the P-E loops.

Table S1: Maximum ΔT observed at a temperature (T), adiabatic temperature change (ΔT), isothermal entropy change (ΔS), applied electric field (ΔE), isothermal heat i.e. refrigerant capacity (Q = ΔTΔS), electrocaloric coefficient (ΔT/ΔE) of typical ferroelectric materials. **Bulk (B) and Film (F)*

EC Materials	T (K)	|ΔT| (K)	|ΔS| (J/kgK)	ΔE (kV/cm)	|Q| (J/kg)	|ΔT/ΔE| (K cm/kV)	Ref.
Lead-based materials							
0.9PMN-0.1PT(B)	298	0.23		105		0.0022	1
0.70PMN–0.30PT (B)	429	2.7	2.3	90	6.21	0.03	2
$PbZr_{0.455}Sn_{0.455}Ti_{0.09}O_3$(B)	317	1.6	1.8	30	54	0.0533	3
0.93PMN–0.07PT (F)	298	9	11	723	99	0.012	4
$PbZrO_3$ (F)	508	11.4		510		0.022	5
$(Pb_{0.97}La_{0.02})(Zr_{0.95}Ti_{0.05})O_3$(F)	210	8.5		1110		0.008	6
$PbZr_{0.95}Ti_{0.05}O_3$(F)	499	12	8	776	96	0.015	7
$PbZr_{0.52}Ti_{0.48}O_3$(F)	659	11.1	6.17	577	68.49	0.0192	8
Polymer-based materials(F)							
P(VDF-TrFE)68/32 mol. %	306	20	95	1600	1900	0.0125	9
P(VDF-TrFE-CFE)	303	15	80	1500	1200	0.011	10
P(VDF-TrFE)/BST75	352	2.5		600		0.0042	11
Terpolymer/PMN-PT	303	31		1800		0.017	12
P(VDF-TrFE) 55/45 mol %	353	12	56	2090	672	0.0057	13
Lead-free materials							
$BaZr_{0.2}Ti_{0.8}O_3$(B)	313	4.5	8	145	36	0.031	14
$SrTiO_3$(B)	17	0.06		70		0.0008	15
$Na_{0.5}Bi_{0.5}TiO_3$(B)	412	0.33	0.45	50	0.1485	0.0066	16
$Ba_{0.65}Sr_{0.35}Ti_{0.997}Mn_{0.003}O_3$(B)	293	3.1	4.8	130	14	0.023	17
$BaTiO_3$ (F)	353	7.1	10.1	800	71.71	0.0089	18
$SrBiTa_2O_9$ (F)	560	4.93	2.4	600	14	0.008	19
BNBT/BCZT bilayer(F)	**370**	**23**	**26.1**	**620**	**600.3**	**0.037**	**This work**

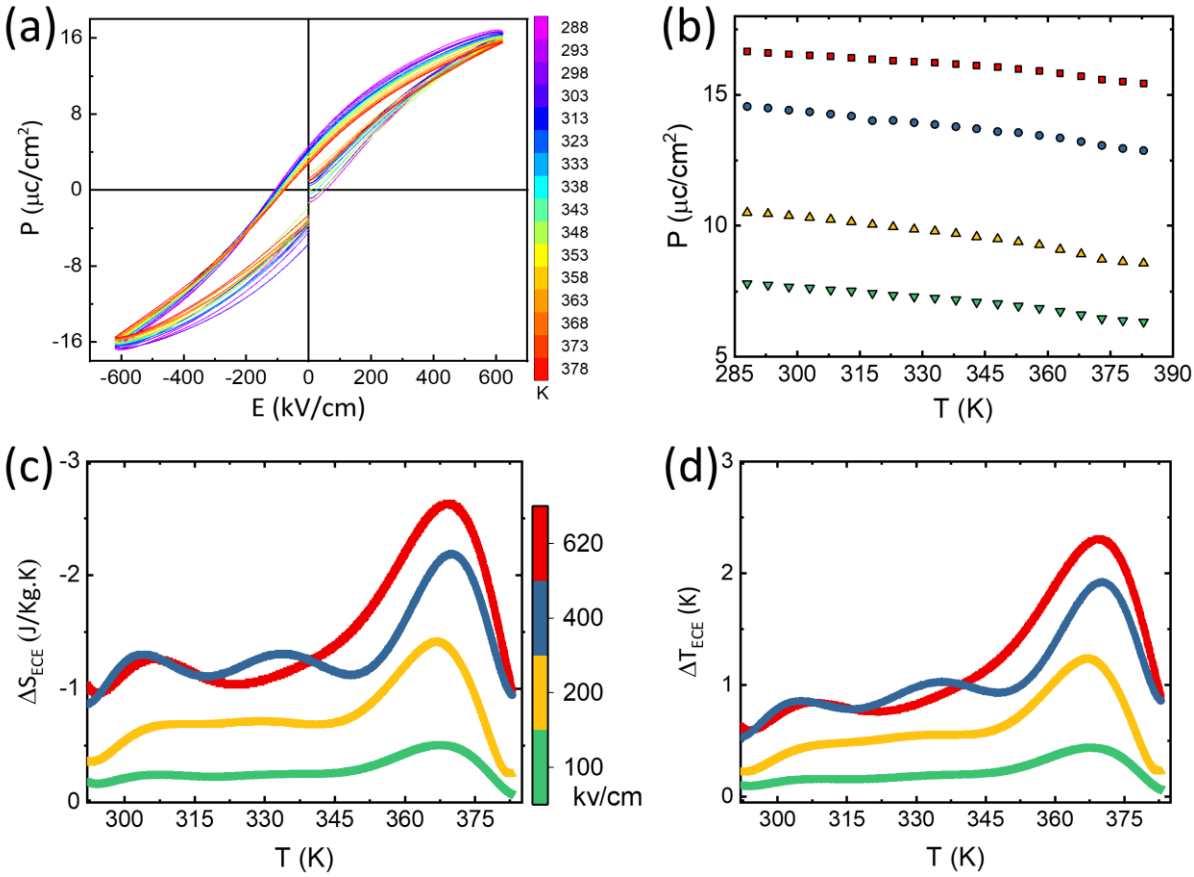

Figure S3: EC results of BCZT$_{400}$ single layer sample. **a,** P-E loops measured as function of temperature under maximum electric field of 620 kV/cm. *measurements were carried out at a fixed frequency of 1 kHz*. **b,** Variation of maximum polarization as a function of temperature under four different electric fields. **c,** Plots of isothermal entropy, ΔS_{ECE}, change vs temperature, and **d,** plots of adiabatic temperature, ΔT_{ECE}, change vs. temperature under four different electric field.

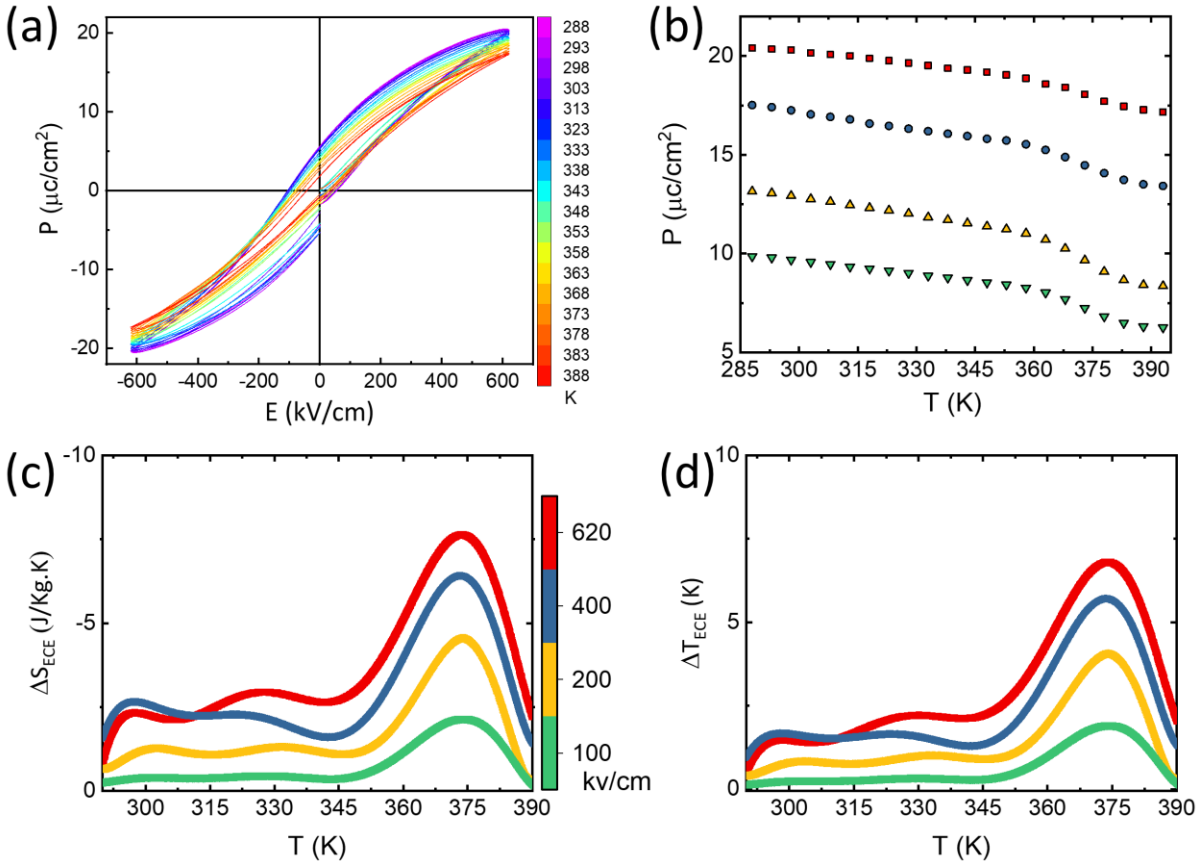

Figure S4: EC results of $BNBT_{40}/BCZT_{360}$ bilayer sample. **a,** P-E loops measured as function of temperature under maximum electric field of 620 kV/cm. *measurements were carried out at a fixed frequency of 1 kHz*. **b,** Variation of maximum polarization as a function of temperature under four different electric fields. **c,** Plots of isothermal entropy, ΔS_{ECE}, change vs temperature, and **d,** plots of adiabatic temperature, ΔT_{ECE}, change vs. temperature under four different electric field.

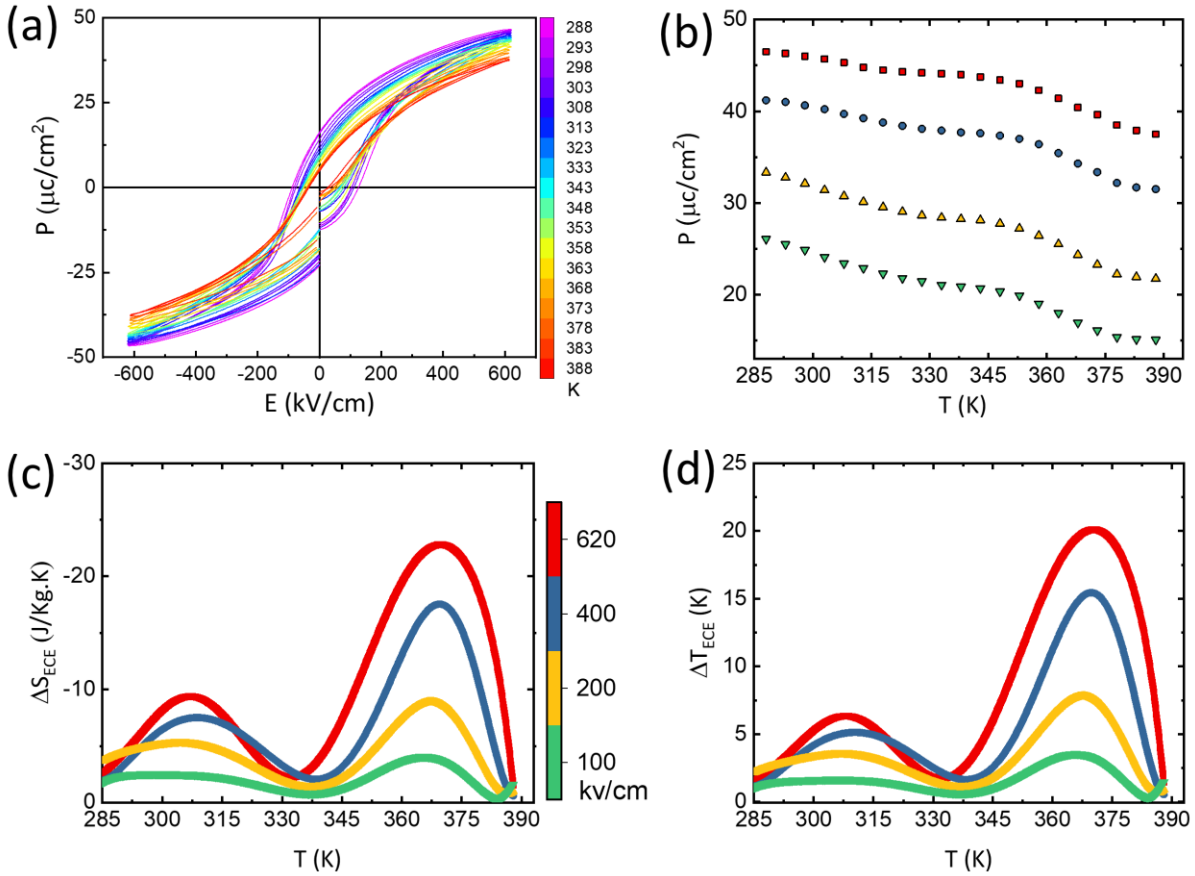

Figure S5: EC results of BNBT$_{300}$/BCZT$_{100}$ bilayer sample. **a,** P-E loops measured as function of temperature under maximum electric field of 620 kV/cm. *measurements were carried out at a fixed frequency of 1 kHz*. **b,** Variation of maximum polarization as a function of temperature under four different electric fields. **c,** Plots of isothermal entropy, ΔS_{ECE}, change vs temperature, and **d,** plots of adiabatic temperature, ΔT_{ECE}, change vs. temperature under four different electric field.

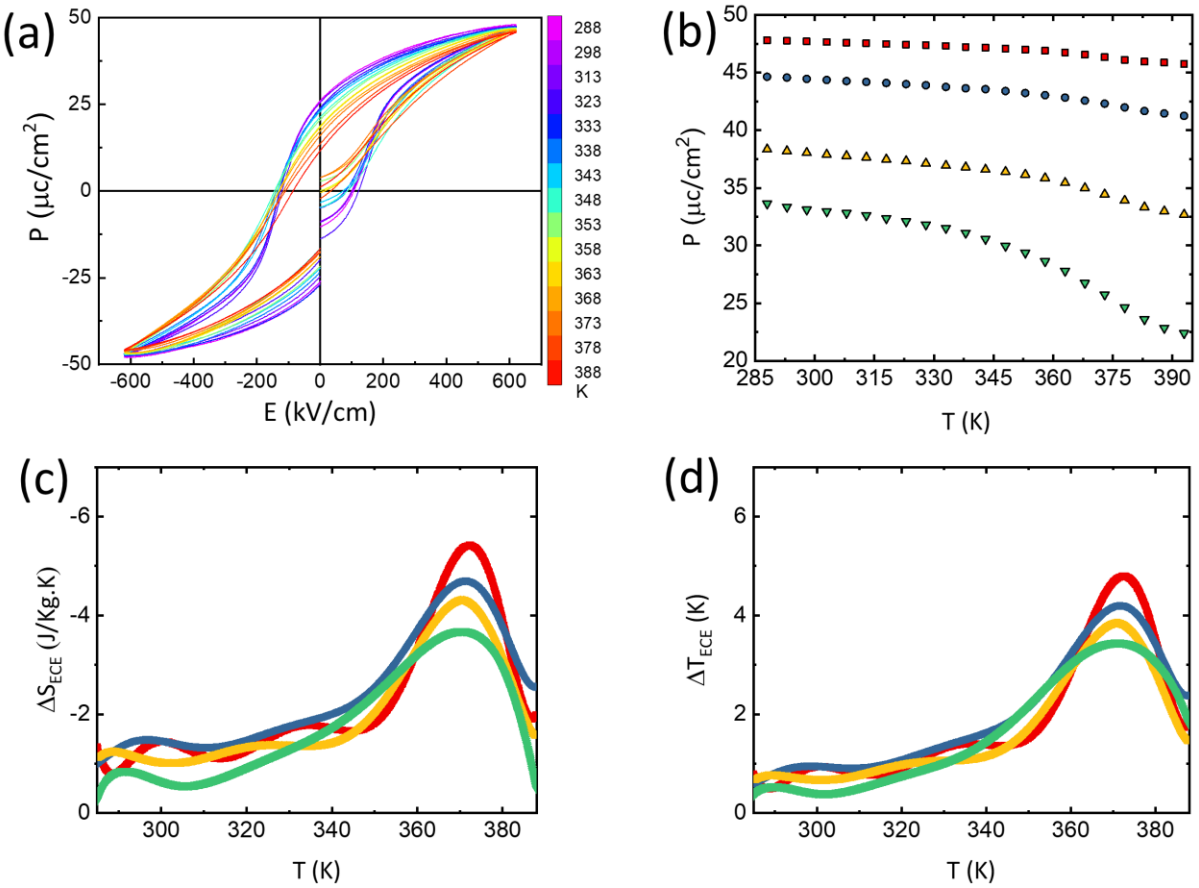

Figure S6: EC results of BNBT$_{400}$ single layer sample. **a,** P-E loops measured as function of temperature under maximum electric field of 620 kV/cm. *measurements were carried out at a fixed frequency of 1 kHz*. **b,** Variation of maximum polarization as a function of temperature under four different electric fields. **c,** Plots of isothermal entropy, ΔS_{ECE}, change vs temperature, and **d,** plots of adiabatic temperature, ΔT_{ECE}, change vs. temperature under four different electric field.

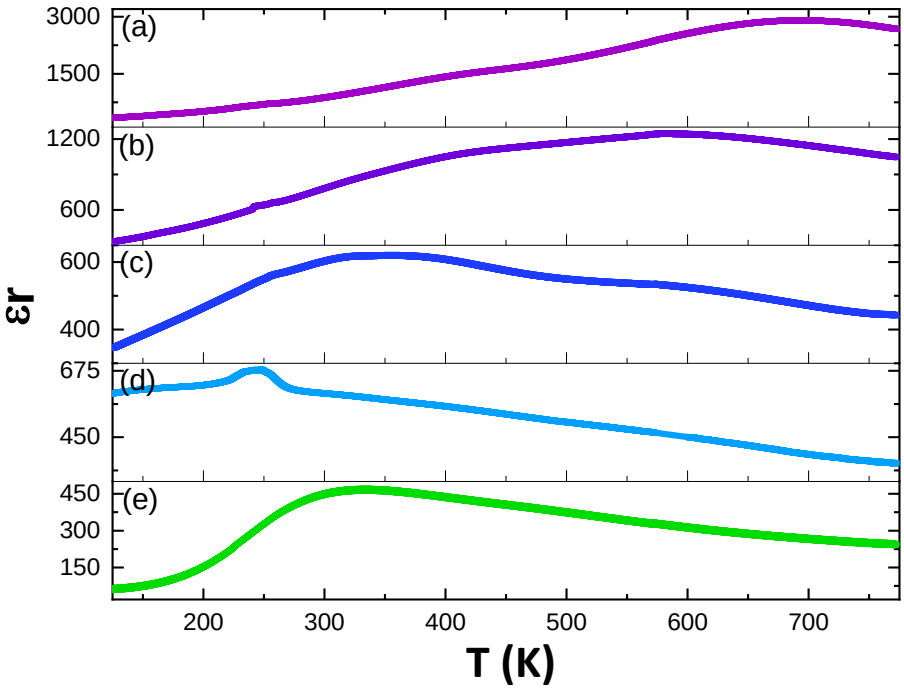

Figure S7: Relative permittivity (ε_r) vs temperature plots measured at 1 kHz in the temperature range 125 to 775 K where **a**, $BNBT_{400}$, **b**, $BNBT_{300}/BCZT_{100}$, **c**,$BNBT_{200}/BCZT_{200}$, **d**, $BNBT_{40}/BCZT_{360}$ and **e**, $BCZT_{400}$.

Figure S7 shows the dielectric permittivity vs temperature plots of the bilayer samples under investigation. The broad maximum permittivity temperature (Tm) and the depolarization temperature (T_d) are observed at ~675 and ~400 K, respectively, for BNBT single layer (Fig. S7(a)), which are consistent with those in previous reports [20, 21]. A broad maximum in permittivity is observed in the temperature range of 300 – 370 K for BCZT single layer (Fig. S7(e)). Both T_m and T_d of BNBT/BCZT bilayer thin films shift to lower temperatures with the decrease in BNBT film thickness (increase in BCZT film thickness). The T_m and T_d of $BNBT_{300}/BCZT_{100}$ bilayer are located around ~390 and ~600 K, respectively. In case of $BNBT_{200}/BCZT_{200}$ bilayer thin film, the highest dielectric permittivity occurs at 315 – 370 K. As the thickness of BCZT approaches to 360 nm ($BNBT_{40}/BCZT_{360}$), the physical properties of the bilayer thin film is expected to be dominated by the BCZT layer. The broad peak of average dielectric constant in all bilayer thin films indicate a diffuse phase transition, which might be due to the interlayer electrostatic interactions.[22, 23]

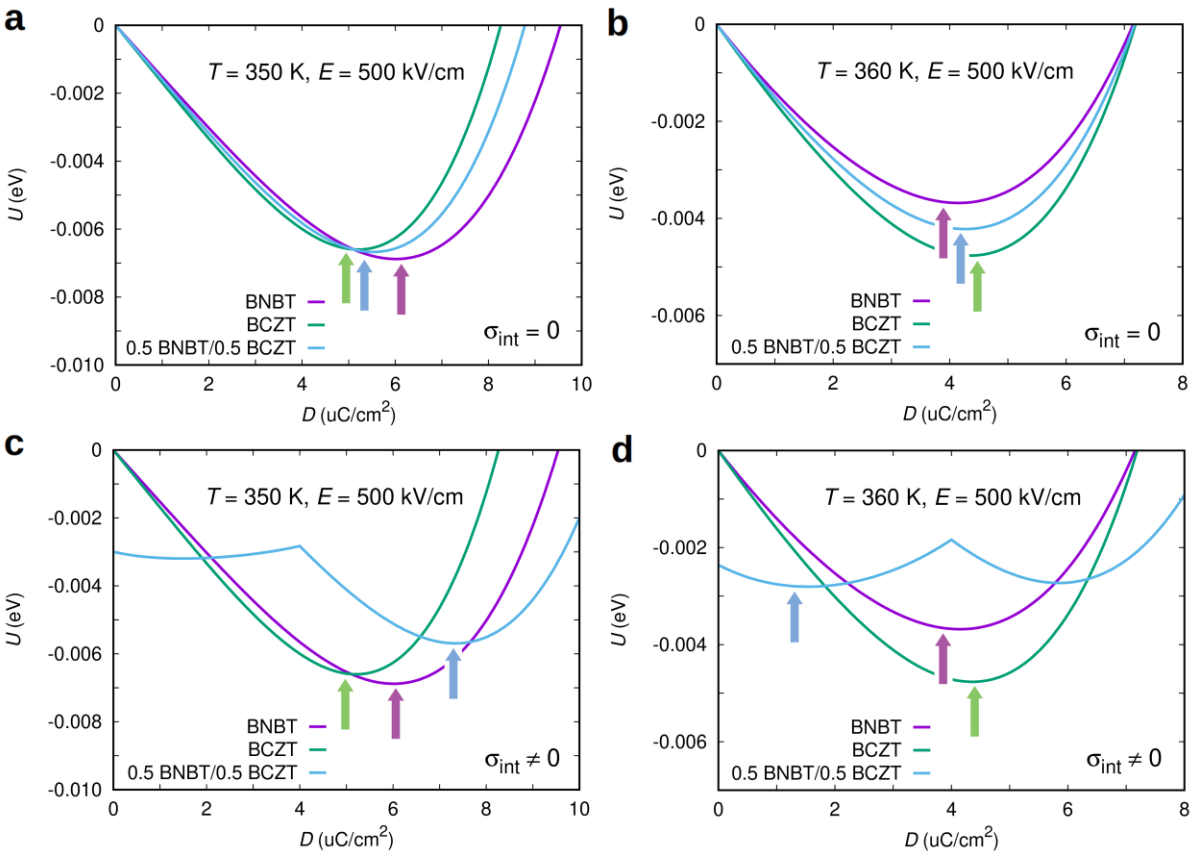

Figure S8: Theoretical calculations for single-domain bulk BNBT, bulk BCZT, and a 0.5 BNBT/ 0.5 BCZT bilayer considering different temperatures and an arbitrary electric field of 500 kV/cm. **a-b** Results obtained for a null interface charge and **c-d** for σ_{int} = 4 μC/cm^2. Coloured arrows indicate spontaneous electric polarisations.

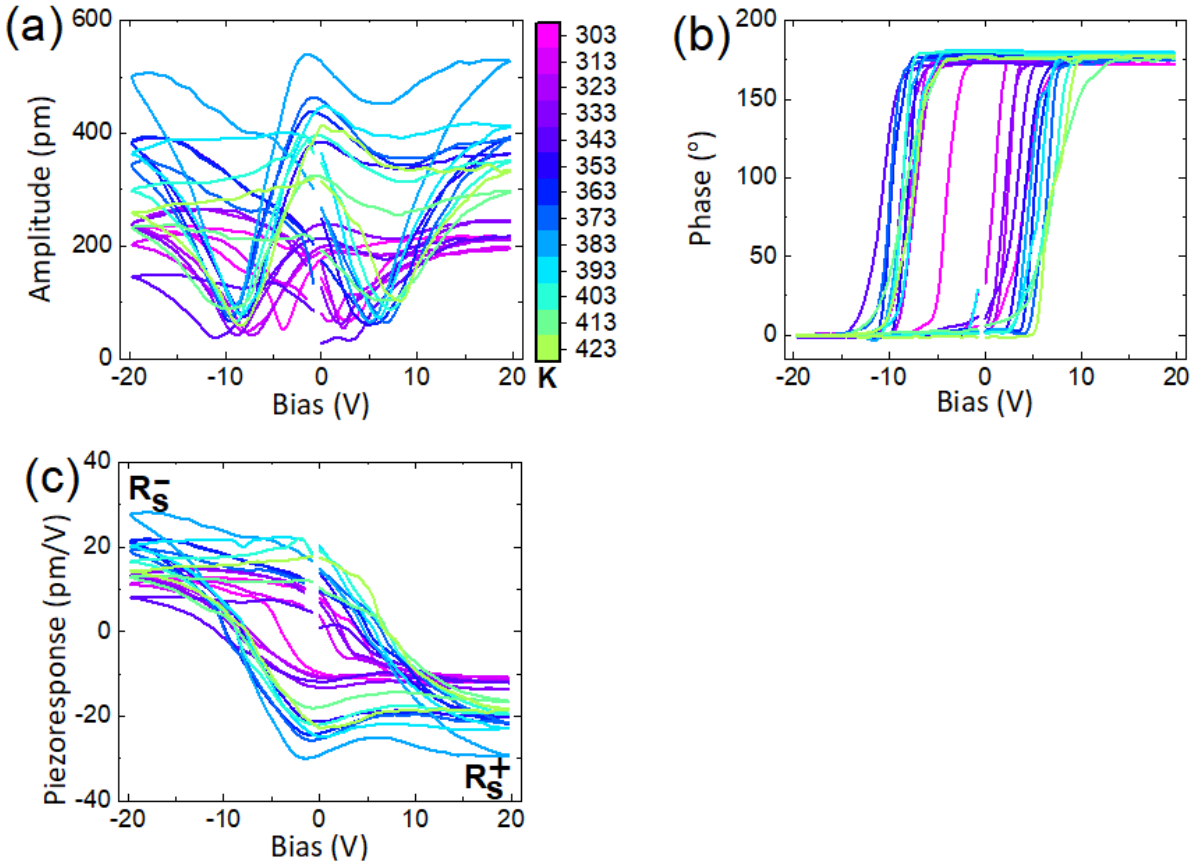

Figure S9: **PFM measurements at different temperatures**. **a**, Amplitude-voltage butterfly loops. **b**, phase-voltage hysteresis loops. **c**, Temperature dependence of piezoresponse against voltage after SHO fitting.

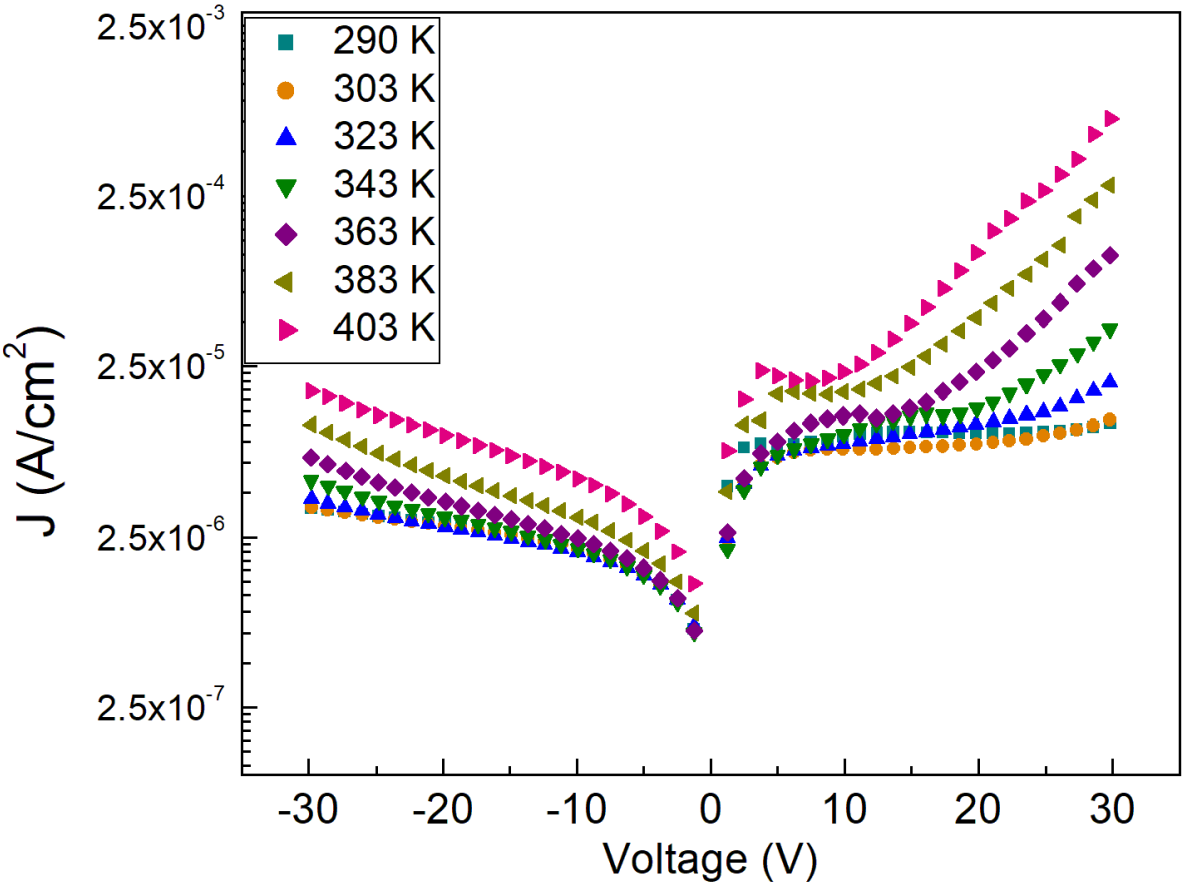

Figure S10: The leakage current density versus voltage curves (I-V) of $BZCT_{200}/BNBT_{200}$ bilayer thin film measured at various temperatures.

Supplementary information references

1 Crossley, S. *et al.* Direct electrocaloric measurement of 0.9 Pb $(Mg_{1/3}Nb_{2/3})O_3$-0.1 $PbTiO_3$ films using scanning thermal microscopy. *Applied Physics Letters* **108**, 032902 (2016).

2 Rožič, B. *et al.* Influence of the critical point on the electrocaloric response of relaxor ferroelectrics. *Journal of Applied Physics* **110**, 064118 (2011).

3 Thacher, P. Electrocaloric effects in some ferroelectric and antiferroelectric Pb (Zr, Ti) O_3 compounds. *Journal of applied physics* **39**, 1996-2002 (1968).

4 Correia, T. *et al.* Investigation of the electrocaloric effect in a $PbMg_{1/3}Nb_{2/3}O_3$-$PbTiO_3$ relaxor thin film (vol 95, 182904, 2009). (2010).

5 Parui, J. & Krupanidhi, S. Electrocaloric effect in antiferroelectric $PbZrO_3$ thin films. *physica status solidi (RRL)–Rapid Research Letters* **2**, 230-232 (2008).

6 Hao, X., Yue, Z., Xu, J., An, S. & Nan, C.-W. Energy-storage performance and electrocaloric effect in (100)-oriented $Pb_{0.97}La_{0.02}(Zr_{0.95}Ti_{0.05})O_3$ antiferroelectric thick films. *Journal of applied physics* **110**, 064109 (2011).

7 Mischenko, A., Zhang, Q., Scott, J., Whatmore, R. & Mathur, N. Giant electrocaloric effect in thin-film $PbZr_{0.95}Ti_{0.05}O_3$. *Science* **311**, 1270-1271 (2006).

8 Chukka, R. *et al.* Enhanced cooling capacities of ferroelectric materials at morphotropic phase boundaries. *Applied Physics Letters* **98**, 242902 (2011).

9 Lu, S. *et al.* Organic and inorganic relaxor ferroelectrics with giant electrocaloric effect. *Applied Physics Letters* **97**, 162904 (2010).

10 Li, X. *et al.* Tunable temperature dependence of electrocaloric effect in ferroelectric relaxor poly (vinylidene fluoride-trifluoroethylene-chlorofluoroethylene terpolymer. *Applied Physics Letters* **99**, 052907 (2011).

11 Jiang, Z. Y., Zheng, X. C. & Zheng, G. P. The enhanced electrocaloric effect in P(VDF-TrFE) copolymer with barium strontium titanate nano-fillers synthesized via an effective hydrothermal method. *RSC Advances* **5**, 61946-61954, (2015).

12 Huang, C., Yang, H.-B. & Gao, C.-F. Giant electrocaloric effect in a cracked ferroelectrics. *Journal of Applied Physics* **123**, 154102, (2018).

13 Neese, B. *et al.* Large Electrocaloric Effect in Ferroelectric Polymers Near Room Temperature. *Science* **321**, 821-823, (2008).

14 Qian, X.-S. *et al.* Giant Electrocaloric Response Over A Broad Temperature Range in Modified BaTiO3 Ceramics. *Advanced Functional Materials* **24**, 1300-1305, (2014).

15 Hegenbarth, E. Studies of the electrocaloric effect of ferroelectricceramics at low temperatures. *Cryogenics* **1**, 242-243, (1961).

16 Bai, Y., Zheng, G.-P. & Shi, S.-Q. Abnormal electrocaloric effect of $Na_{0.5}Bi_{0.5}TiO_3$–$BaTiO_3$ lead-free ferroelectric ceramics above room temperature. *Materials Research Bulletin* **46**, 1866-1869, (2011).

17 Liu, X. Q., Chen, T. T., Wu, Y. J. & Chen, X. M. Enhanced Electrocaloric Effects in Spark Plasma-Sintered $Ba_{0.65}Sr_{0.35}TiO_3$-Based Ceramics at Room Temperature. *Journal of the American Ceramic Society* **96**, 1021-1023, (2013).

18 Bai, Y., Han, X., Ding, K. & Qiao, L.-J. Combined effects of diffuse phase transition and microstructure on the electrocaloric effect in $Ba_{1-x}Sr_xTiO_3$ ceramics. *Applied Physics Letters* **103**, 162902, (2013).

19 Chen, H., Ren, T.-L., Wu, X.-M., Yang, Y. & Liu, L.-T. Giant electrocaloric effect in lead-free thin film of strontium bismuth tantalite. *Applied Physics Letters* **94**, 182902, (2009).

20 Tanaka, Y. *et al.* High electromechanical strain and enhanced temperature characteristics in lead-free (Na,Bi)TiO(3)-BaTiO(3) thin films on Si substrates. *Scientific reports* **8**, 7847-7847, (2018).

21 Cordero, F., Craciun, F., Trequattrini, F., Mercadelli, E. & Galassi, C. Phase transitions and phase diagram of the ferroelectric perovskite $(Na_{0.5}Bi_{0.5})_{1-x}Ba_xTiO_3$by anelastic and dielectric measurements. *Physical Review B* **81**, 144124, (2010).
22 Roytburd, A. L., Zhong, S. & Alpay, S. P. Dielectric anomaly due to electrostatic coupling in ferroelectric-paraelectric bilayers and multilayers. *Applied Physics Letters* **87**, 092902, (2005).
23 Maurya, D., Sun, F. C., Alpay, S. P. & Priya, S. A new method for achieving enhanced dielectric response over a wide temperature range. *Sci Rep* **5**, 15144, (2015).